CAMBRIDGE
UNIVERSITY PRESS

Article

Gysinite-(La), PbLa(CO₃)₂(OH)·H₂O, a new rare earth mineral of the ancylite group from the Saima alkaline complex, Liaoning Province, China

Bin Wu[1]* ⬤, Xiang-ping Gu[2] ⬤, Can Rao[3], Ru-cheng Wang[4], Xing-qing Xing[5], Jian-jun Wan[1], Fu-jun Zhong[1] and Christophe Bonnetti[1]

[1]State Key Laboratory of Nuclear Resources and Environment, East China University of Technology, Nanchang, Jiangxi 330013, China; [2]School of Geosciences and Info-physics, Central South University, Changsha, Hunan 410083, China; [3]School of Earth Sciences, Zhejiang University, Hangzhou, Zhejiang 310027, China; [4]State Key Laboratory for Mineral Deposits Research, School of Earth Sciences and Engineering, Nanjing University, Nanjing, Jiangsu 210033, China; and [5]No. 241 Group Co., Ltd., Liaoning Geological Exploration and Mining Group, Fengcheng, Liaoning 118119, China

Abstract

The new mineral, gysinite-(La), with the ideal formula $PbLa(CO_3)_2(OH){\cdot}H_2O$, has been discovered in lujavrite from the Saima alkaline complex, Liaoning Province, China. It commonly occurs as subhedral to anhedral, granular and platy crystals of 5 to 50 μm in size, in interstices or enclosed in microcline, aegirine and nepheline. Associated minerals include nepheline, aegirine, microcline, natrolite, eudialyte, lamprophyllite, bastnäsite-(Ce), parasite-(Ce), ancylite-(La), ancylite-(Ce), bobtraillite, britholite-(Ce), thorite, calcite and galena. The crystallisation of gysinite-(La) may be related to the post-magmatic carbonation event. Gysinite-(La) crystals are generally transparent, colourless, or pale yellow, with a vitreous lustre and white streak. It is brittle with an uneven fracture, and the estimated Mohs hardness is 3½ to 4. The calculated density is 5.007 g/cm³. Optically, gysinite-(La) is biaxial (–), α= 1.832(2), β= 1.849(4), γ = 1.862(5) in white light and $2V_{meas} = 81.6°$. The empirical formula of gysinite-(La) is $(La_{0.93}Pb_{0.61}Nd_{0.23}Pr_{0.14}Sr_{0.04}Gd_{0.02}Sm_{0.01}Eu_{0.01}Ca_{0.01})_{\Sigma2}(CO_3)_2$ $(OH)_{1.34}{\cdot}0.66H_2O$, which is calculated on the basis of general formula $(REE_xM^{2+}_{2-x})(CO_3)_2(OH)_x{\cdot}(2-x)H_2O$. The strongest eight lines of its powder X-ray diffraction pattern [*d*, Å (*I*, %) (*hkl*)] are: 5.596 (21) (011), 4.349 (100) (110), 3.732 (68) (111), 2.984 (61) (121), 2.667 (21) (031), 2.363 (48) (131), 2.090 (29) (221) and 2.028 (21) (212). Gysinite-(La) is orthorhombic, in the space group *Pmcn*, and unit-cell parameters refined from single-crystal X-ray diffraction data are: *a* = 5.0655(2) Å, *b* = 8.5990(3) Å, *c* = 7.3901(4) Å, *V* = 321.90(2) Å³ and *Z* = 2. It is a new member of the ancylite group and isostructural with gysinite-(Nd), but with La and Pb dominant in the metal cation sites in the structure.

Introduction

The new mineral, gysinite-(La), with the ideal formula $PbLa$ $(CO_3)_2(OH){\cdot}H_2O$, has been discovered in lujavrite from the Saima alkaline complex, Liaoning Province, northeast China. For the past few decades, the Saima complex has been mined, initially for its uranium resource. Since 2015 it has also been explored for Nb and rare earth element (REE) resources by the China Geological Survey (CGS) and No. 241 Group Co., Ltd., Liaoning Geological Exploration and Mining Group. This alkaline complex is also the type locality for gugiaite, hezuolinite, fengchengite and newly approved fluorsigaiite (Peng *et al.*, 1962; Yang *et al.*, 2012; Shen *et al.*, 2017; Wu *et al.*, 2022a).

This new mineral is the La-dominant analogue of the approved mineral gysinite-(Nd), $PbNd(CO_3)_2(OH){\cdot}H_2O$, therefore the naming of gysinite-(La) is in consistency with rules of the International Mineralogical Association, Commission on New Minerals, Nomenclature and Classification (IMA–CNMNC) for rare earth minerals and dominant constituents (Levinson, 1966; Bayliss and Levinson, 1988; Hatert and Burke, 2008). Gysinite-(La) is the ninth member of the ancylite-group minerals with the general formula $(REE_xM^{2+}_{2-x})(CO_3)_2(OH)_x{\cdot}(2-x)H_2O$, where REE = La, Ce and Nd, and *M* = Ca, Sr and Pb (Table 1). The species and the name gysinite-(La) with symbol Gys-La have been approved by the Commission on New Minerals, Nomenclature and Classification of the International Mineralogical Association (IMA2022-008, Wu *et al.*, 2022b). The type material is deposited at the Geological Museum of China, No. 15 Yangrouhutong, Xisi, Beijing 100031, PR China, with catalogue number M16133.

Occurrence and paragenesis

The Saima alkaline complex (longitude E120°16', latitude N40°58') is located in the eastern Liaodong Peninsula within the north-eastern

*Author for correspondence: Bin Wu, Email: wubin@ecut.edu.cn

Table 1. Characteristics of the ancylite-group minerals with the general formula $(REE_xM^{2+}_{2-x})(CO_3)_2(OH)_x\cdot(2-x)H_2O$.

Series /Species	Formula	S.g.	Unit cell parameters				Z	Bond distances (Å)		Density (g/cm³)
			a (Å)	*b* (Å)	*c* (Å)	*V* (Å³)		*M*–O	C–O	
Ancylite										
Ancylite-(La)[a]	LaSr(CO₃)₂(OH)·H₂O	*Pmcn*	5.044	8.541	7.292	314.15	2	2.622	1.280	3.69
Ancylite-(Ce)[b]	CeSr(CO₃)₂(OH)·H₂O	*Pmcn*	5.030	8.530	7.290	312.42	2	2.615	1.283	4.15
Calcioancylite										
Calcioancylite-(La)[c]	(LaCa)(CO₃)₂(OH)·H₂O	*Pmcn*	5.025	8.515	7.272	311.17	2	n.a.	n.a.	n.a.
Calcioancylite-(Ce)[d]	(Ce,Ca,Sr)(CO₃)₂(OH)·H₂O	*Pmcn*	5.010	8.501	7.267	309.40	2	2.620	1.240	3.95
Calcioancylite-(Nd)[e]	Nd₂.₈Ca₁.₂(CO₃)₂(OH)·H₂O	*Pm*11	4.976	8.468	7.212	303.89	2	2.578	1.297	4.08
Gysinite										
Gysinite-(La)*	PbLa(CO₃)₂(OH)·H₂O	*Pmcn*	5.066	8.599	7.390	321.90	2	2.635	1.286	5.01
Gysinite-(Nd)[f]	PbNd(CO₃)₂(OH)·H₂O	*Pmcn*	5.003	8.555	7.239	309.83	2	2.595	1.285	4.82
Kozoite										
Kozoite-(La)[g]	La(CO₃)(OH)	*Pmcn*	4.986	8.513	7.227	306.70	4	n.a.	n.a.	4.16
Kozoite-(Nd)[h]	Nd(CO₃)(OH)	*Pmcn*	4.983	8.519	7.257	308.50	4	2.614	1.301	4.77

n.a. = not available; S.g. = space group.

References: [a]Petersen *et al.* (2001); [b]Dal Negro *et al.* (1975); [c]Wang *et al.* (2022); [d]Belovitskaya *et al.* (2013); [e]Orlandi *et al.* (1990); [f]Chabot and Sarp (1985); [g]Miyawaki *et al.* (2003); [h]Miyawaki *et al.* (2000); *this study.

segment of the North China Craton. This complex is primarily composed of phonolite, nepheline syenite, lujavrite and alkaline pegmatite, with a coeval emplacement age ranging from 224 to 230 Ma (Wu *et al.*, 2010; Zhu *et al.*, 2016). Nepheline syenite and lujavrite intruded the Cambrian–Ordovician limestone and Precambrian marble. These Saima alkaline rocks were derived from the low-degree partial melting of subcontinental lithospheric mantle, which was metasomatised by melts or fluids from recycled ancient continental crust (Zhu *et al.*, 2017). The various suits of rocks composing the Saima batholith were then emplaced as a result of crustal assimilation and fractional crystallisation processes (Zhu *et al.*, 2016). Post-magmatic metasomatism such as albitisation, skarnification and carbonation were widespread. The petrography and mineralogy of the Saima complex have been described in detail in previous studies (Wu *et al.*, 2015, 2016; Zhu *et al.*, 2016).

In lujavrite, gysinite-(La) occurs as either single subhedral to anhedral, granular and platy crystals from 5 to 50 μm in size in a matrix of nepheline and microcline (Fig. 1a,b), or as aggregates consisting of a few crystals individually <20 μm in fractures or interstices of nepheline, aegirine and microcline (Fig. 1c). In a few cases, compositionally heterogeneous zoning, probably caused by variable Pb and REE contents, can be observed in crystals under back-scattered electron imaging (Fig. 1d). Associated minerals include nepheline, aegirine, microcline, natrolite, eudialyte, lamprophyllite, bastnäsite-(Ce), parasite-(Ce), ancylite-(La), ancylite-(Ce), bobtraillite, britholite-(Ce), thorite, calcite and galena. In the same lujavrite sample, most of eudialyte grains are partly to completely replaced by an unidentified Pb-bearing zirconosilicate (potentially PbZrSi₃O₉·2H₂O based on our unpublished data). The occurrence of gysinite-(La) associated with Ca-rich wall rocks (limestone and marble) allows us to propose that crystallisation of gysinite-(La) may be related to a post-magmatic carbonation event within the Saima complex.

Physical and optical properties

Individual granular or platy crystals of gysinite-(La) are transparent, colourless or pale yellow in transmitted light with a white coloured streak and vitreous lustre. It shows no fluorescence under either longwave or shortwave ultraviolet light. Optically, gysinite-(La) is biaxial (–), α= 1.832(2), β= 1.849(4), γ = 1.862(5) (white light)

and $2V_{meas} = 81.6°$. Pleochroism was not observed. Some of its physical properties could not be determined due to its small grain size. Gysinite-(La) is brittle, with an uneven fracture, and has a Mohs hardness value of ∼ 3½ to 4. No cleavage twinning or parting was observed. The calculated density is 5.007 g/cm³ based on the empirical formula and refined single-crystal unit-cell parameters (see below). Gysinite-(La) is non-magnetic with respect to a neodymium magnet, and soluble in 30% HCl (aq) at room temperature. According to the calculated density and the measured indices of refraction, the compatibility index $[1 - (K_P/K_C)]$ is –0.011, and corresponds to the 'superior' category (Mandarino, 1981).

Raman spectroscopy

A Raman spectrum was obtained from a randomly oriented gysinite-(La) grain, by a Renishaw inVia RM2000 spectrometer equipped with a 50× Leica objective lens at the State Key Laboratory of Nuclear Resources and Environment, East China University of Technology. The excitation wavelength was 532 nm, and the laser output power was set at 20 mW. The spatial resolution was estimated to be 1 μm, and the spectral resolution was 1 cm⁻¹. High-pure silicon with a 520 cm⁻¹ Raman shift was chosen for calibration. The spectrum was collected from 100 to 4000 cm⁻¹ and the accumulation time for each spectrum was ∼30 s with 2–3 accumulations.

The Raman characteristics for the carbonate unit are clearly observed in Fig. 2. The strongest Raman band at 1077 cm⁻¹ is assigned to the intense symmetric C–O stretching mode (ν_1) and relatively weak bands at 700 and 726 cm⁻¹ correspond to the C–O asymmetric in-plane bending modes (ν_4) (Bühn *et al.*, 1999; Buzgar and Apopei, 2009; Chakhmouradian and Dahlgren, 2021). The C–O out-of-plane bending signals (ν_2) at 870–880 cm⁻¹, which occur in some anhydrous carbonates, are not observed in gysinite-(La). In addition, a weak line at 1443 cm⁻¹ is probably assigned to the C–O ν_3 asymmetric stretching mode, which is also observed in bastnäsite and aragonite-group minerals (Frost and Dickfos, 2007; Buzgar and Apopei, 2009), and lines around 1738 cm⁻¹ may be regarded as the combination bands of $\nu_1 + \nu_4$ modes (Gunasekaran *et al.*, 2006). The bands of H₂O present at 3249 and 3549 cm⁻¹ correspond to the O–H asymmetric and symmetric ν_1 stretching modes, respectively, and the band at 1612 cm⁻¹ is assigned to the O–H ν_2
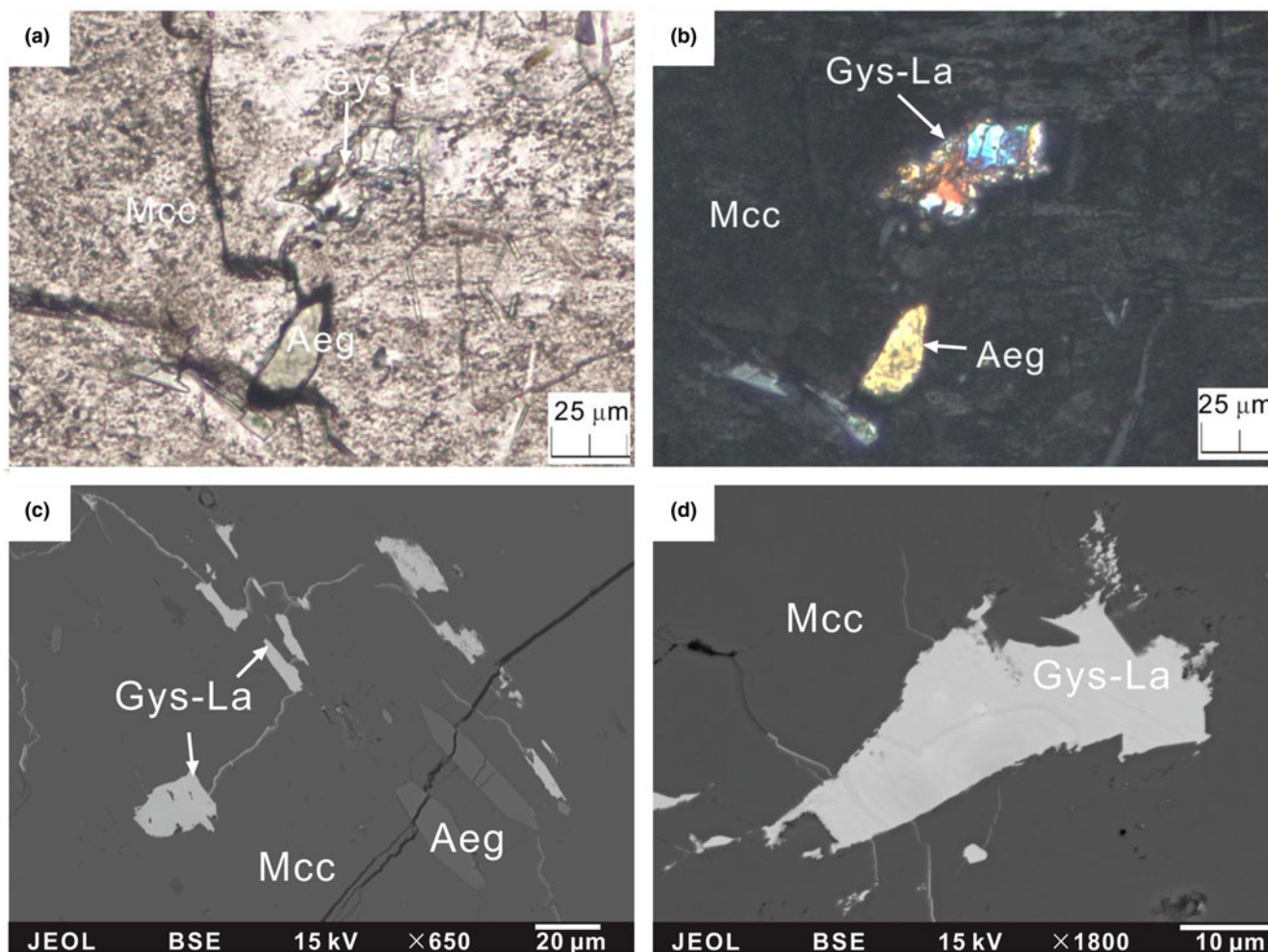
Fig. 1. Photomicrographs (a,b) and back-scattered electron images (c,d) showing the occurrence of gysinite-(La). (a,b) Gysinite-(La) and aegirine crystals in microcline under parallel nicols (a) and crossed nicols (b) in transmitted light. (c) Aggregate of gysinite-(La) crystals in interstices of microcline (including holotype crystal selected for Raman spectroscopy). (d) Single gysinite-(La) crystal showing weak heterogeneous zoning. Mineral abbreviations: Aeg – aegirine, Gys-La – gysinite-(La), Mcc – microcline. Specimen #SM01.

bending mode (Carey and Korenowski, 1998). The Raman bands at the lowest region of the spectrum including 167, 379 and 567 cm^{-1} can be attributed to the lattice modes.

Chemical composition

Quantitative elemental microanalysis of gysinite-(La) was conducted with a JEOL-JXA 8530F Plus electron microprobe in wavelength dispersive spectroscopy mode at 15 kV and 50 nA, with a defocused beam diameter of 5 μm to minimise diffusion of elements mobile under the electron beam, at the State Key Laboratory of Nuclear Resources and Environment, East China University of Technology. Measurement time for each element on peaks and background was 20 and 10 s, respectively. Standards for calibration were fluorapatite ($CaK\alpha$ and $FK\alpha$), celestine ($SrL\alpha$), crocoite ($PbL\alpha$), monazite ($LaL\alpha$, $CeL\alpha$, $PrL\beta$ and $NdL\alpha$), and synthetic REE-phosphates ($SmL\alpha$, $EuL\alpha$ and $GdL\alpha$). The F content in gysinite-(La) was below detection limits of the EPMA (i.e. ≤ 500 ppm), hence it is not listed in Table 2. According to the general formula $(REE_xM^{2+}_{2-x})(CO_3)_2(OH)_x(2-x)H_2O$ of ancylite-group minerals, the empirical formula of gysinite-(La) is:

$(La_{0.93}Pb_{0.61}Nd_{0.23}Pr_{0.14}Sr_{0.04}Gd_{0.02}Sm_{0.01}Eu_{0.01}Ca_{0.01})_{\Sigma 2}(CO_3)_2 (OH)_{1.34}\cdot 0.66H_2O$. The OH group was calculated from the stoichiometry, and the number of water molecules was calculated based on the sum of $(OH+H_2O) = 2$ atoms per formula unit (apfu). The ideal formula, in line with gysinite-(Nd), becomes $PbLa(CO_3)_2(OH)\cdot H_2O$, which requires PbO 44.51, La_2O_3 32.53, CO_{2calc} 17.56, H_2O_{calc} 5.40, total 100 (all in wt.%).

Powder X-ray diffraction determination

The powder X-ray diffraction pattern (XRD) of gysinite-(La) was collected on a Rigaku XtaLAB Synergy diffractometer ($CuK\alpha$, λ = 1.54184 Å) in powder Gandolfi mode at 50 kV and 1 mA, at the School of Earth Sciences and Info-physics, Central South University, China. The structural model of a single crystal (see below) was used to index the powder XRD pattern of gysinite-(La) (Table 3). The strongest eight lines of the powder XRD pattern [d in Å (I) (hkl), Fig. 3] were: 5.596 (21) (011), 4.349 (100) (110), 3.732 (68) (111), 2.984 (61) (121), 2.667 (21) (031), 2.363 (48) (131), 2.090 (29) (221) and 2.028 (21) (212). The unit cell parameters were refined in an orthorhombic crystal system using the program *UnitCell* (Holland and Redfern, 1997)
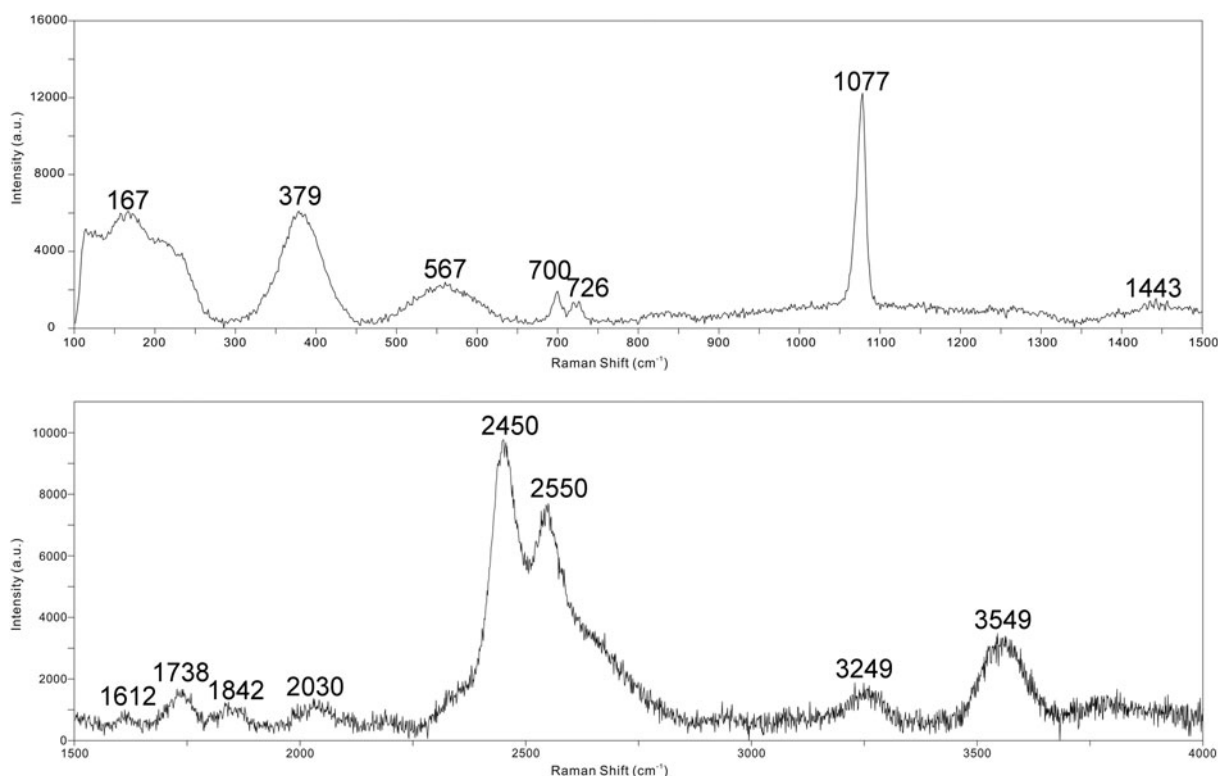
Fig. 2. Raman spectrum for gysinite-(La).

Table 2. Composition from electron microprobe data (in wt.%) for gysinite-(La).

Constituent	Mean	Range	S.D.	apfu	Probe standard
CaO	0.08	0.04–0.14	0.03	0.007	Fluorapatite
SrO	0.71	0.26–1.22	0.37	0.036	Celestine
PbO	28.66	26.57–30.53	1.01	0.613	Crocoite
La$_2$O$_3$	31.80	28.79–35.78	2.61	0.930	Monazite
Ce$_2$O$_3$	0.05	bdl–0.18	0.06	0.001	Monazite
Pr$_2$O$_3$	5.03	4.07–6.26	0.78	0.145	Monazite
Nd$_2$O$_3$	7.96	6.28–9.80	1.18	0.226	Monazite
Sm$_2$O$_3$	0.53	bdl–0.98	0.35	0.015	Synthetic REE-phosphate
Eu$_2$O$_3$	0.38	0.04–0.64	0.18	0.010	Synthetic REE-phosphate
Gd$_2$O$_3$	0.64	0.45–0.93	0.15	0.017	Synthetic REE-phosphate
CO$_2$*	18.46	18.17–18.78	0.16	2.000	
H$_2$O$^\#$	7.27	7.15–7.39	0.06	1.344(OH)+0.656H$_2$O	
Total	101.57	100.27–102.67	0.70		

S.D. = standard deviation; bdl = below detection limits.
*CO$_2$ was assumed as 2 apfu according to the general formula of the ancylite group, and $^\#$(OH+H$_2$O) was assumed as 2 apfu and each of them was calculated based on the charge balance.

and are: $a = 5.0591(2)$ Å, $b = 8.5899(3)$ Å, $c = 7.3987(4)$ Å, $V = 321.52(2)$ Å^3 and $Z = 2$.

Crystal structure refinement

Single-crystal X-ray diffraction data were collected at room temperature on a $10 \times 10 \times 10$ μm crystal fragment dug from a polished thin section, using a Rigaku XtaLAB Synergy diffractometer, at the School of Earth Sciences and Info-physics, Central South University, China, which was equipped with CuKα radiation ($\lambda = 1.54184$ Å) at working conditions of 50 kV and 1mA, respectively. The diffraction data were treated with the program *CrysAlis^Pro* (Rigaku Oxford Diffraction, UK) and the structure of gysinite-(La) was refined using the software *SHELX*

(Sheldrick, 2015a, 2015b). Once all atoms were located, they were refined anisotropically and the occupancies of La, Pb, Nd, Pr and Sr at the metal cation site were manually adjusted according to the chemical composition, yielding:

(La$_{0.90}$Pb$_{0.66}$Nd$_{0.24}$Pr$_{0.16}$Sr$_{0.04}$)$_{\Sigma 2}$(CO$_3$)$_2$(OH)$_2$, without further consideration for H$_2$O. The crystal structure refinement finally converged to $R_1 = 3.21\%$ for 360 unique reflections ($I > 2\sigma(I)$) and 34 parameters. Unit cell parameters refined from these reflections are $a = 5.0655(2)$ Å, $b = 8.5990(3)$ Å, $c = 7.3901(4)$ Å, $V = 321.90(2)$ Å^3 and $Z = 2$, in the space group *Pmcn*. See Table 4 for details of data collection and refinement. Atom coordinates, anisotropic atomic displacement parameters and site population are given in Tables 5–6, and selected bond distances and angles in Table 7. The bond-valence sums of atoms,

Table 3. Experimental and calculated* powder X-ray diffraction data (*d* in Å, *I* in %) for gysinite-(La).

I_{obs}	I_{calc}	d_{obs}	d_{calc}	h k l
21	**38**	**5.596**	**5.606**	**0 1 1**
100	**100**	**4.349**	**4.359**	**1 1 0**
68	**58**	**3.732**	**3.756**	**1 1 1**
18	41	3.389	3.398	0 1 2
61	**21**	**2.984**	**2.994**	**1 2 1**
4	6	2.793	2.803	0 2 2
21	**27**	**2.667**	**2.670**	**0 3 1**
17	28	2.529	2.530	2 0 0
10	17	2.446	2.452	1 2 2
48	**49**	**2.363**	**2.362**	**1 3 1**
4	8	2.182	2.180	2 2 0
10	11	2.149	2.147	0 4 0
29	**44**	**2.090**	**2.091**	**2 2 1**
21	**37**	**2.028**	**2.029**	**2 1 2**
8	9	1.916	1.910	1 4 1
4	10	1.840	1.836	2 3 1
11	4	1.741	1.753	1 3 3
4	8	1.653	1.655	3 1 0
4	8	1.629	1.627	1 5 0
4	9	1.597	1.598	2 4 1
4	6	1.559	1.558	0 5 2
8	4	1.535	1.536	3 2 1
8	14	1.501	1.503	2 3 3
4	5	1.469	1.471	2 1 4
5	7	1.429	1.426	3 3 1
6	2	1.397	1.396	2 5 1
9	9	1.325	1.327	2 5 2
5	8	1.291	1.291	1 6 2
3	2	1.249	1.248	3 4 2
1	6	1.230	1.224	2 2 5
6	2	1.219	1.218	0 4 5

*The calculated values were obtained using *VESTA 3* (Momma and Izumi, 2011).
The strongest values are given in bold.

Table 4. Data collection and structure refinement details for gysinite-(La).

Crystal data	
Ideal formula	$PbLa(CO_3)_2(OH) \cdot H_2O$
Crystal dimensions (mm)	$0.010 \times 0.010 \times 0.010$
Crystal system, space group	Orthorhombic, *Pmcn*
Temperature (K)	296(2)
a (Å)	5.0655(2)
b (Å)	8.5990(3)
c (Å)	7.3901(4)
V (Å³)	321.90(2)
Z	2
Calculated density (g·cm⁻³)	5.007(2)
Data collection	
Crystal description	Colourless granular crystal
Instrument	Rigaku XtaLAB Synergy
Working voltage (kV) and current (mA)	50, 1
Radiation type, wavelength (Å)	Cu*K*α, 1.54184
Absorption coefficient, μ (mm⁻¹)	103.159
F(000)	414
θ range (°)	7.906 to 77.109
No. of measured, independent and observed [*I* >2σ(*I*)] reflections	2007, 379, 360
R_{int}	0.0511
Indices range of *h*, *k*, *l*	$-6 \leq h \leq 6$
	$-10 \leq k \leq 8$
	$-9 \leq l \leq 9$
Refinement	
Refinement method	Full-matrix least squares on F^2
Number of reflections, restraints, parameters	379, 0, 34
R_1 [*I* > 2σ(*I*)], R_1(all)	0.0321, 0.0352
wR_2 [*I* > 2σ(*I*)], wR_2(all)*	0.0778, 0.0792
GoF	1.094
$\Delta\rho_{max}$, $\Delta\rho_{min}$ (e⁻ Å⁻³)	1.44, −1.45

*$wR_2 = \{\sum[w(F_o^2 - F_c^2)^2]/\sum[w(F_o^2)^2]\}^{1/2}$; $w = 1/[\sigma^2(F_o)^2 + (aP)^2 + bP]$ where *a* is 0.036, *b* is 6.13 and *P* is $[2F_c^2 + Max(F_o^2, 0)]/3$.

calculated using the parameters given by Brese and O'Keeffe (1991) are presented in Table 8. The structure is illustrated in Fig. 4. The crystallographic information file has been deposited with the Principal Editor of *Mineralogical Magazine* and is available as Supplementary material (see below).

Gysinite-(La) is a new Pb-analogue of the ancylite-group minerals and it is isostructural with gysinite-(Nd), but with the dominance of La over Nd in the REE occupancy (Dal Negro *et al.*, 1975; Sarp and Bertrand, 1985). In the ancylite structure, the cations REE (i.e. La, Ce and Nd) and *M* (i.e. Ca, Sr and Pb) occupy the same coordinated site, which is bonded to eight
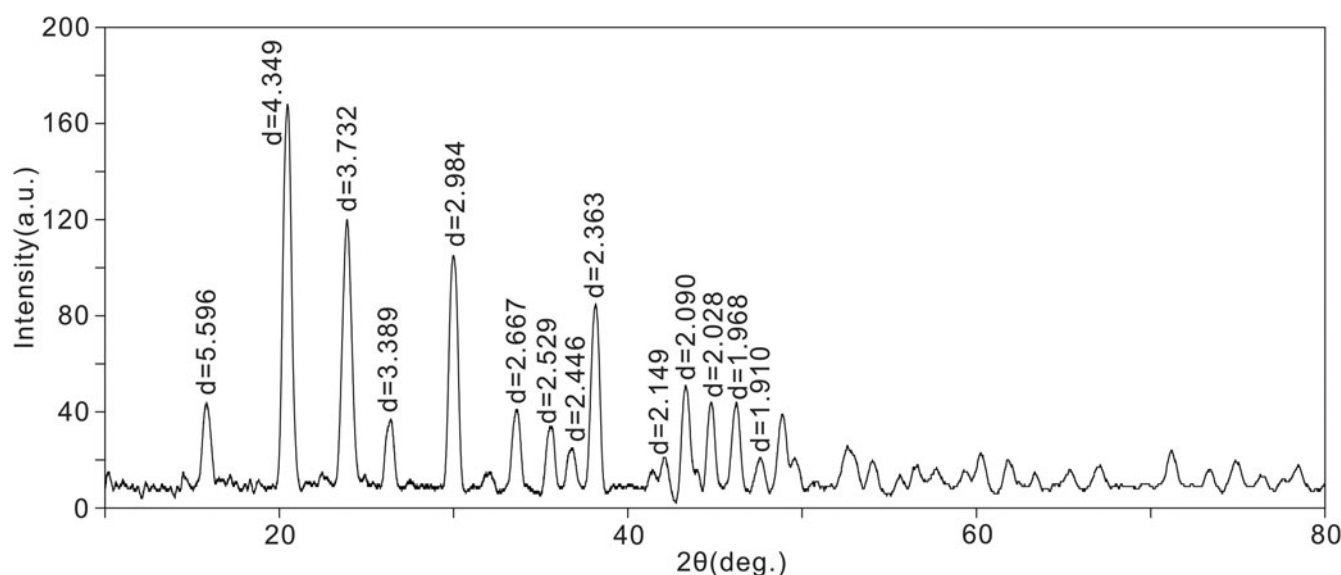

Fig. 3. Powder X-ray diffraction pattern for gysinite-(La).

Table 5. Wyckoff positions, inferred site populations, fractional coordinates of atoms, and equivalent isotropic displacement parameters in gysinite-(La) structure.

Atom	Wyckoff position	x	y	z	Site population	$U_{(eq)}$
M	4c	¾	0.66131(7)	0.84875(8)	$La_{0.45}Pb_{0.33}Nd_{0.12}Pr_{0.08}Sr_{0.02}$	0.0176(3)
C1	4c	¼	0.8090(13)	0.6873(16)	$C_{1.00}$	0.009(2)
O1	4c	¼	0.6825(11)	0.7738(16)	$O_{1.00}$	0.027(2)
O2	8d	0.4703(13)	0.8781(7)	0.6476(9)	$O_{1.00}$	0.0197(13)
O3	4c	¾	0.5905(12)	0.5277(14)	$O_{1.00}$	0.032(2)

Table 6. Anisotropic atomic displacements ($Å^2$) for gysinite-(La).

Atom	U^{11}	U^{22}	U^{33}	U^{23}	U^{13}	U^{12}
M	0.0141(4)	0.0191(4)	0.0196(4)	0.0021(2)	0	0
C1	0.007(5)	0.009(4)	0.011(5)	0.006(4)	0	0
O1	0.022(5)	0.019(4)	0.039(6)	0.007(4)	0	0
O2	0.013(3)	0.021(3)	0.025(3)	0	–0.002(3)	–0.005(3)
O3	0.043(6)	0.034(5)	0.017(5)	–0.004(4)	0	0

Table 8. Calculated bond valence sums (in vu) of atoms for gysinite-(La), using the parameters of Brese and O'Keeffe ([1991]).*

	M	C1	Σ	Theoretical Σ
O1	$0.291^{×2↓×2→}$	$1.412^{×1↓×1→}$	1.995	2
O2	$0.257^{×2↓×1→}$	$1.281^{×2↓×1→}$	1.955	2
	$0.235^{×2↓×1→}$			
	$0.181^{×2↓×1→}$			
O3	$0.440^{×1↓×1→}$		0.816	0.667
	$0.375^{×1↓×1→}$			
Σ	2.747	3.974		
Theoretical Σ	2.667	4		

*Bond valence sums were calculated with the site population factors given in Table 5. The theoretical number of vu of M and O3 is calculated based on ⅔REE³⁺+⅓M^{2+} and ⅔OH+⅓H_2O, respectively, according to its empirical formula for charge balance.

Table 7. Selected bond distances (Å) and angles (°) for gysinite-(La).

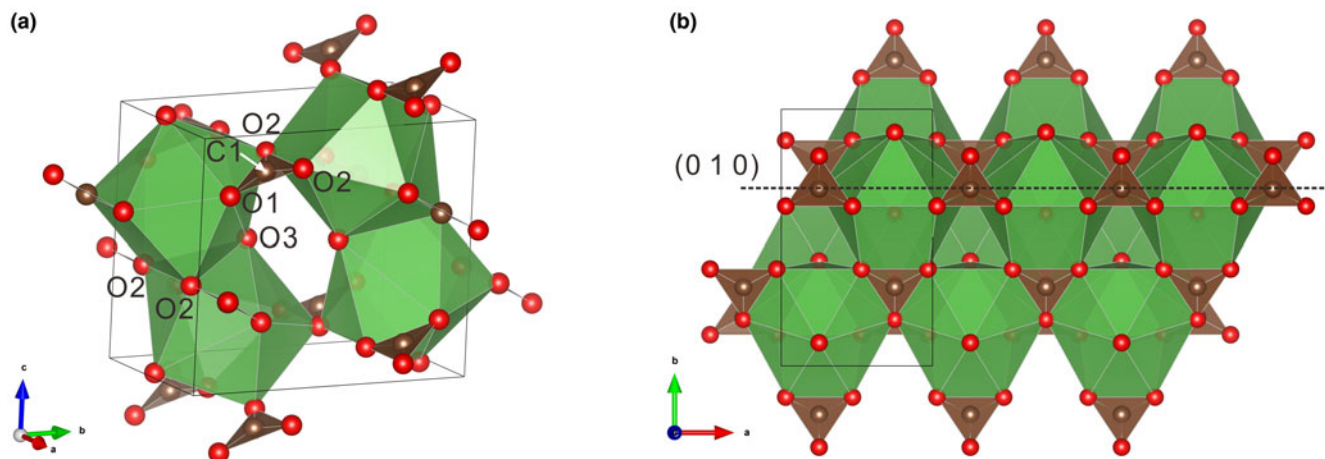| C–O triangle		M–O polyhedron	
C1–O1	1.262(15)	M–O1 ×2	2.599(3)
C1–O2 ×2	1.298(9)	M–O2 ×2	2.646(7)
<C–O>	1.286	M –O2 ×2	2.679(7)
		M–O2 ×2	2.773(7)
		M–O3	2.449 (11)
		M–O3	2.511(11)
		<M–O>	2.635
Angles			
O2–C1–O2	118.6(11)	O1–M–O1	154.1(5)
O1–C1–O2 ×2	120.6(6)	O2–M–O2	49.2(3), 64.8(3), 69.6(3), 95.63(15)
Average	119.9	O3–M–O3	136.2(3)
		O2–M–O3	140.1(2), 70.7(2), 77.5(3)
		O1–M–O3	93.0(2), 79.1(3)
		O1–M–O2	70.4(3), 135.1 (3)
		M–O1–M	154.1(5)
		M–O2–M	95.0(2), 144.9 (3)

oxygen atoms belonging to the CO_3 group and two hydroxyls and water molecules (Dal Negro *et al.*, 1975). According to the chemical composition and occupancy at the metal cation site (i.e. REE and *M*), the ancylite group minerals can be further divided into ancylite–calcioancylite–gysinite–kozoite solid solutions (Miyawaki *et al.*, 2000, 2003). In the gysinite-(La) structure, the ten-fold coordinated *M* cation is mainly dominated by La and Pb over other REE and alkaline-earth elements. The basic framework of gysinite-(La) is composed mainly of *M*–O polyhedra connected with each other by face (O2–O2–O3 triangle) and corner (O2) sharing modes (Fig. 4a). The *M*–O distances vary from 2.599 to 2.773 Å for the eight oxygen atoms ($O1^{×2}$ and $O2^{×6}$) belonging to CO_3 group, whereas the *M*–O3 distances connected to the hydroxyls are shorter (2.449 and 2.511 Å). The mean *M*–O bond distance of 2.635 Å is slightly longer than that in gysinite-(Nd) (2.595 Å, Chabot and Sarp, 1985). The carbon atom at the C1 site in gysinite-(La) structure is bonded to 3 O atoms ($O1^{×1}$ and $O2^{×2}$) to form isolated isosceles triangles with an average C–O bond distance of 1.286 Å. The C–O triangle and *M*–O polyhedron form layer-like units parallel to (0 1 0) with OH and H_2O located between layers (Fig. 4b).

Fig. 4. Crystal structure of gysinite-(La) (unit cell outlined in black lines) plotted with *VESTA 3* (Momma and Izumi, 2011). (a) *M*–O polyhedron (green) connected with each other by face (O2–O2–O3 triangle) and corner (O2) sharing modes. (b) The C–O triangle (brown) and *M*–O polyhedron form layer-like units parallel to (0 1 0).

Comparative data from ancylite-(La) to gysinite-(La) in Table 1 illustrate that the progressive substitution of Ca and Sr (effective ionic radius 1.23 and 1.36 Å, respectively, Shannon, 1976) by Pb (effective ionic radius 1.40 Å) in the crystal structure leads to an increase in average M–O bond distance from 2.622 to 2.635 Å, as well as increases in the unit-cell parameters and density.

The bond-valence sums of 2.747 valence units (vu) for the M-site in gysinite-(La) is close to its theoretical value of 2.667 vu, which was calculated on the basis of ⅔REE^{3+} and ⅓M^{2+} in accordance with its empirical formula. The bond valence sums for the O1, O2 and O3 sites are 1.995, 1.955 and 0.816 vu, respectively. Similarly, the 0.816 vu for O3 is close to its theoretical value of 0.667 vu, calculated on the basis of ⅔OH and ⅓H$_2$O at the O3 site for charge balance. In comparison with O1 and O2, the lower bond-valence for O3 suggests a mixed occupancy by hydroxyl and water molecules, which is also demonstrated by its actual composition and Raman spectroscopy.

Implications

Gysinite-(La) is the second Pb-analogue of the ancylite group ever discovered after gysinite-(Nd) (Chabot and Sarp, 1985; Sarp and Bertrand, 1985). Regardless of being from different rock types, both gysinite-(La) and gysinite-(Nd) were crystallised in hydrothermal conditions. Gysinite-(Nd) was discovered as a secondary mineral after uraninite alteration in the Shinkolobwe sediment-hosted uranium-polymetallic deposit of Congo, and in hydrothermal lead-zinc deposits of Italy and Germany (Sarp and Bertrand, 1985; Olmi and Sabelli, 1991), whereas gysinite-(La) was discovered in altered lujavrite from the Saima alkaline complex of China. Rare earth elements in gysinite-(La) were most likely to have been derived from the alteration and decomposition of eudialyte, which was ultimately replaced by another unidentified Pb-bearing zirconosilicate during a post-magmatic carbonation event associated with Sr–Pb-rich hydrothermal fluids. The altered lujavrite is also the co-type sample for recently approved fluorsigaiite with the ideal formula of Ca$_2$Sr$_3$(PO$_4$)$_3$F (Wu *et al.*, 2022a), which similarly occurs in interstices of aegirine, microcline and nepheline, and was most probably also crystallised from late hydrothermal events. This Sr–Pb-rich carbonation event affecting the Saima alkaline system has been documented in our previous work – it induced the intense replacement of primary wadeite and rinkite-(Ce) by a series of secondary hydrothermal minerals including Sr-bearing calcite and strontianite (Wu *et al.*, 2015, 2019). However, although country rocks such as limestone and marble could be a candidate for such Sr–Pb-rich carbonation fluids, the true source of Sr and Pb in the hydrothermal fluids, responsible for the crystallisation of gysinite-(La) and other Sr–Pb-rich minerals, remains to be determined.

The discoveries of gysinite-(La) and gysinite-(Nd) suggest that in addition to Sr and Ca, Pb could occur as another conventional bivalent cation in the M site of the ancylite-group structure. Lead and Ba are actually common constituents in carbonate minerals, as exampled by the Ca, Sr, Pb and Ba analogue of aragonite-group minerals with general formula M^{2+}(CO$_3$) (De Villiers, 1971; Negro and Ungaretti, 1971). Therefore, it may be considered that the discovery of gysinite-(La) draws attention to a certain expectation that the Ba analogue of the ancylite group, as well as the Ce analogue of gysinite will be discovered in the future.

References

Bayliss P. and Levinson A.A. (1988) A system of nomenclature for rare-earth mineral species: revision and extension. *American Mineralogist*, **73**, 422–423.

Belovitskaya Y.V., Pekov I.V., Gobechiya E.R. and Kabalov Y.K. (2013) Refinement of the crystal structure of calcioancylite-(Ce) by the Rietveld method. *Crystallography Reports*, **58**, 216–219.

Brese N.E. and O'Keeffe M. (1991) Bond-valence parameters for solids. *Acta Crystallographica*, **B47**, 192–197.

Bühn B., Rankin A.H., Radtke M., Haller M. and Knöchel A. (1999) Burbankite, a (Sr,REE,Na,Ca)-carbonate in fluid inclusions from carbonatite-derived fluids: Identification and characterization using Lase Raman spectroscopy, SEM-EDX and synchrotron micro-XRF analysis. *American Mineralogist*, **84**, 1117–1125.

Buzgar N. and Apopei A.I. (2009) The Raman study of certain carbonates. *Geologie*, **55**, 97–112.

Carey D.M. and Korenowski G.M. (1998) Measurement of the Raman spectrum of liquid water. *Journal of Chemical Physics*, **108**, 2669–2675.

Chabot B. and Sarp H. (1985) Structure refinement of Gysinite La$_{0.16}$Nd$_{1.18}$Pb$_{0.66}$(CO$_3$)$_2$(OH)$_{1.34}$·0.66 H$_2$O. *Zeitschrift fur Kristallographie*, **171**, 155–158.

Chakhmouradian A.R. and Dahlgren S. (2021) Primary inclusions of burbankite in carbonatites from the Fen complex, southern Norway. *Mineralogy and Petrology*, **115**, 161–171.

Dal Negro A., Rossi G. and Tazzoli V. (1975) The crystal structure of ancylite, (RE)$_x$(Ca,Sr)$_{2-x}$(CO$_3$)$_2$(OH)$_x$·(2–x)H$_2$O. *American Mineralogist*, **60**, 280–284.

De Villiers J.P.R. (1971) Crystal structures of aragonite, strontianite, and witherite. *American Mineralogist*, **56**, 758–767.

Frost R.L. and Dickfos M.J. (2007) Raman spectroscopy of halogen-containing carbonates. *Journal of Raman Spectroscopy*, **38**, 1516–1522.

Gunasekaran S., Anbalagan G. and Pandi S. (2006) Raman and infrared spectra of carbonates of calcite structure. *Journal of Raman Spectroscopy*, **37**, 892–899.

Hatert F. and Burke E.A.J. (2008) The IMA-CNMNC dominant-constituent rule revisited and extended. *The Canadian Mineralogist*, **46**, 717–728.

Holland T.J.B. and Redfern S.A.T. (1997) Unit cell refinement from powder diffraction data: the use of regression diagnostics. *Mineralogical Magazine*, **61**, 65–77.

Levinson A. (1966) A system of nomenclature for rare-earth minerals. *American Mineralogist*, **51**, 152.

Mandarino J.A. (1981) The Gladstone-Dale relationship: part IV. The compatibility concept and its application. *The Canadian Mineralogist*, **19**, 441–450.

Miyawaki R., Matsubara S., Yokoyama K., Takeuchi K., Nakai I. and Terada Y. (2000) Kozoite-(Nd), Nd(CO$_3$)(OH), a new mineral in an alkali olivine basalt from Hizen-cho, Saga Prefecture, Japan. *American Mineralogist*, **85**, 1076–1081.

Miyawaki R., Matsubara S., Yokoyama K., Iwano S., Hamasaki K. and Yukinori I. (2003) Kozoite-(La), La(CO$_3$)(OH), a new mineral from Mitsukoshi, Hizen-cho, Saga Prefecture, Japan. *Journal of Mineralogical and Petrological Sciences*, **98**, 137–141.

Momma K. and Izumi F. (2011) VESTA 3 for three-dimensional visualization of crystal, volumetric and morphology data. *Journal of Applied Crystallography*, **44**, 1272–1276.

Negro A. and Ungaretti L. (1971) Refinement of the crystal structure of aragonite. *American Mineralogist*, **56**, 768–772.

Olmi F. and Sabelli C. (1991) Gysinite-(Nd), a mineral new to Italy, from Sa Duchessa, Sardinia. *Neues Jahrbuch für Mineralgie-Monatshefte*, **4**, 185–191.

Orlandi P., Pasero M. and Vezzalini G. (1990) Calcioancylite-(Nd), a new REE-carbonate from Baveno, Italy. *European Journal of Mineralogy*, **2**, 413–418.

Peng Q.R., Cao R.L., Zou Z.R., Zhang L.J., Yin S.S. and Ding K.S. (1962) Gugiaite, $Ca_2BeSi_2O_7$, a new beryllium mineral belonging to the melilite group. *Acta Geologica Sinica*, **42**, 259–274 [in Chinese with English abstract].

Petersen O.V., Niedermayr G., Gault R.A., Brandsttter F. and Giester G. (2001) Ancylite-(La) from the Ilímaussaq alkaline complex, South Greenland: Contribution to the mineralogy of Ilímaussaq, no. 106. *Neues Jahrbuch für Mineralogie-Monatshefte*, **11**, 493–504.

Sarp H. and Bertrand J. (1985) Gysinite, $Pb(Nd,La)(CO_3)_2(OH)\cdot H_2O$, a new lead, rare-earth carbonate from Shinkolobwe, Shaba, Zaïre and its relationship to ancylite. *American Mineralogist*, **70**, 1314–1317.

Shannon R.D. (1976) Revised effective ionic radii and systematic studies of interatomic distances in halides and chalcogenides. *Acta Crystallographica*, **A32**, 751–767.

Sheldrick G.M. (2015a) SHELXT – Integrated space-group and crystal structure determination. *Acta Crystallographica*, **A71**, 3–8.

Sheldrick G.M. (2015b) Crystal structure refinement with SHELX. *Acta Crystallographica*, **C71**, 3–8.

Shen G.F., Xu J.S., Yao P. and Li G.W. (2017) Fengchengite: a new species with the Na-poor but vacancy-dominant $N(5)$ site in the eudialyte group. *Acta Mineralogica Sinica*, **37**, 140–151 [in Chinese with English abstract].

Wang Y.J., Gu X.P., Dong G.C., Hou Z.Q., Yang Z.S., Fan G., Wang Y.F., Tang C., Cheng Y.H. and Qu K. (2022) Calcioancylite-(La), IMA 2021-090. CNMNC Newsletter 65. *Mineralogical Magazine*, **86**, https://doi.org/10.1180/mgm.2022.14

Wu F.Y., Yang Y.H., Marks M.A.W., Liu Z.C., Zhou Q., Ge W.C., Yang J.S., Zhao Z.F., Mitchell R.H. and Markl G. (2010) In situ U–Pb, Sr, Nd and Hf isotopic analysis of eudialyte by LA-(MC)-ICP-MS. *Chemical Geology*, **273**, 8–34.

Wu B., Wang R.C., Yang J.H., Wu F.Y., Zhang W.L., Gu X.P. and Zhang A.C. (2015) Wadeite ($K_2ZrSi_3O_9$), an alkali-zirconosilicate from the Saima agpaitic rocks in northeastern China: its origin and response to multi-stage activities of alkaline fluids. *Lithos*, **224–225**, 126–142.

Wu B., Wang R.C., Yang J.H., Wu F.Y., Zhang W.L., Gu X.P. and Zhang A.C. (2016) Zr and REE mineralization in sodic lujavrite from the Saima alkaline complex, northeastern China: A mineralogical study and comparison with potassic rocks. *Lithos*, **262**, 232–246.

Wu B., Wen H.J., Bonnetti C., Wang R.C., Yang J.H. and Wu F.Y. (2019) Rinkite-(Ce) in the nepheline syenite pegmatite from the Saima alkaline complex, northeastern China: its occurrence, alteration, and implications for REE mineralization. *The Canadian Mineralogist*, **57**, 903–924.

Wu B., Gu X.P., Rao C., Wang R.C., Zhong F.J. and Wan J.J. (2022a) Fluorsigaiite, IMA 2021-087a. CNMNC Newsletter 67; *Mineralogical Magazine*, **86**, https://doi.org/10.1180/mgm.2022.56

Wu B., Gu X.P., Rao C., Wang R.C., Xing X.Q., Wan J.J. and Zhong F.J. (2022b) Gysinite-(La), IMA 2022-008. CNMNC Newsletter 67; *Mineralogical Magazine*, **86**, https://doi.org/10.1180/mgm.2022.56

Yang Z.M., Giester G., Ding K.S. and Tillmanns E. (2012) Hezuolinite, $(Sr, REE)_4Zr(Ti,Fe^{3+},Fe^{2+})_2Ti_2O_8(Si_2O_7)_2$, a new mineral species of the chevkinite group from Saima alkaline complex, Liaoning Province, NE China. *European Journal of Mineralogy*, **24**, 189–196.

Zhu Y.S., Yang J.H., Sun J.F., Zhang J.H. and Wu F.Y. (2016) Petrogenesis of coeval silica-saturated and silica-undersaturated alkaline rocks: Mineralogical and geochemical evidence from the Saima alkaline complex, NE China. *Journal of Asian Earth Sciences*, **117**, 184–207.

Zhu Y.S., Yang J.H., Sun J.F. and Wang H. (2017) Zircon Hf-O isotope evidence for recycled oceanic and continental crust in the sources of alkaline rocks. *Geology*, **45**, 407–410.